New-Generation Interferometric Polarimetry

Ivan Martí-Vidal

Onsala Space Observatory

Chalmers University of Technology (Sweden)

QU-ESO Workshop

Munich (October 2017)

Outline

- New Observational Windows.
  - Wide bandwidths, extreme sensitivity, high frequencies.
- Rotation Measure on the Widest Bandwidths.
  - RM Synthesis, RM CLEAN, and super-Gaussian modelling.
- Beating the Dynamic Range.
  - Primary-beam Muller deconvolution.
  - Rotation-invariant CLEANing.
  - Calibration artifacts: Dterms and cross-pol gains. Monte Carlo assessment.
- The Highest Sensitivities.
  - Differential polarimetry.
- The Highest Angular Resolutions.
  - Limitations of the "classical" pol. calibration.
  - Fractional polarizations in Fourier domain.
  - Wide bandwidths (linear polarizers) in VLBI.

Observational Windows

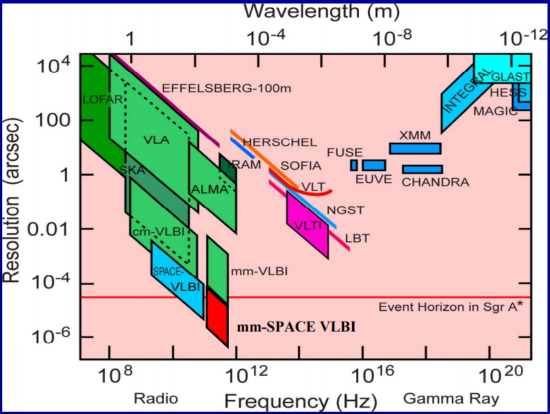

New frequency & resolution windows with high sensitivities & wide BW (e.g., several GHz at ALMA, VLA, VLBI; fract. BW of $\sim$ 1 at LOFAR).

Wide Bandwidth Polarimetry

Wide Bandwidth Polarimetry

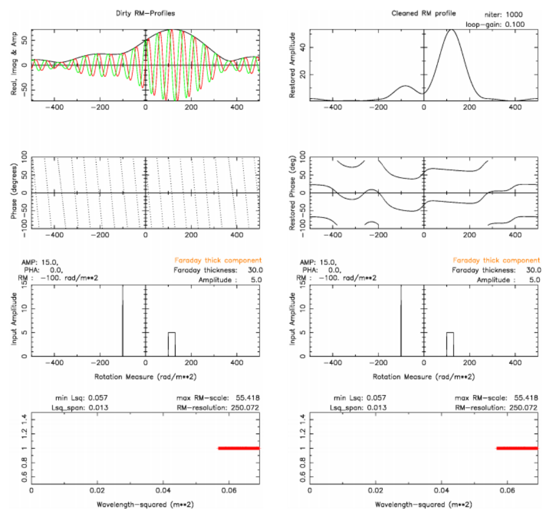

RM Synthesis and RM CLEAN (Raja 2016; based on Brentjens & de Bruyn 2005; Heald 2008).

Wide Bandwidth Polarimetry

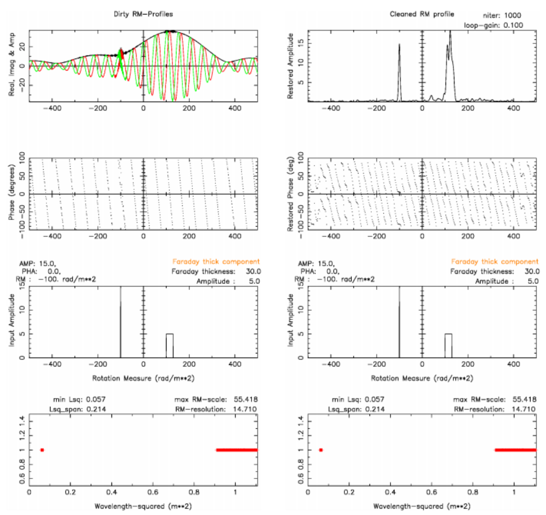

RM Synthesis and RM CLEAN (Raja 2016; based on Brentjens & de Bruyn 2005; Heald 2008).

Wide Bandwidth Polarimetry

$$p(\phi) = -\frac{A}{\sqrt{2\pi}\,\sigma_\phi} \exp\left(2i\psi_0 + \frac{-|\phi - \phi_{\rm peak}|^N}{2\sigma_\phi^N}\right)$$

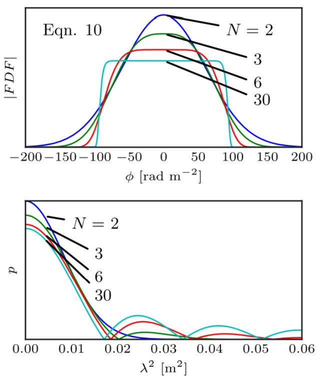

Faraday-thick structures (conceptually similar to MS CLEAN).
Anderson et al. (2017)

Wide Bandwidth Polarimetry

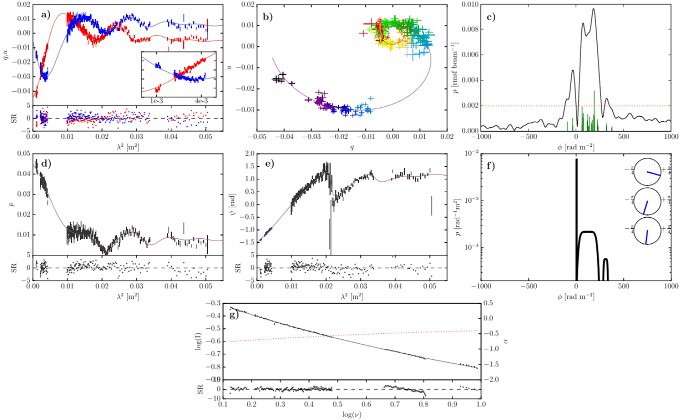

Faraday-depth reconstruction (Anderson et al. 2017)

High Dynamic Range Polarimetry

High Dynamic Ranges: Primary Beam

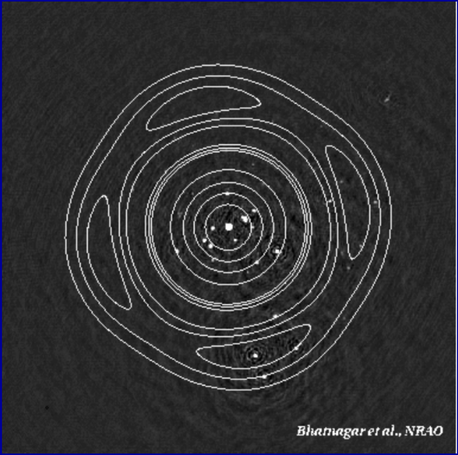

High Dynamic Ranges: Primary Beam

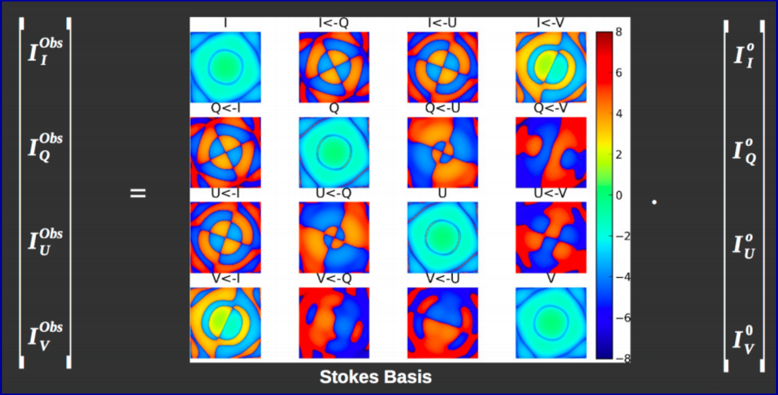

Mueller decomposition of beam response (Bhatnagar 2016).

High Dynamic Ranges: CLEANing Biases

CHALMERS
UNIVERSITY OF TECHNOLOGY

This is ATCA data of a polarised radio galaxy from (Pratley, Johnston-Hollitt et al. 2013)

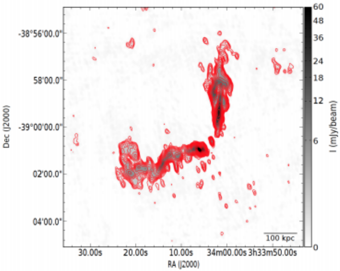

This is the CLEAN components for the source on an Argand diagram. Why are the majority of the components along the axes?

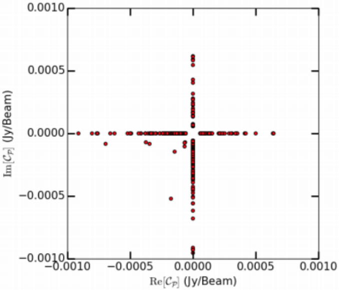

CLEAN in *IQUV* space limits the dynamic range of *m* (Johnston & Hollitt 2016).

High Dynamic Ranges: CLEANing Biases

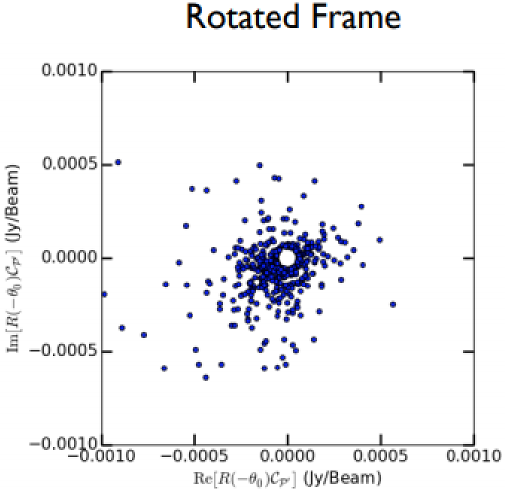

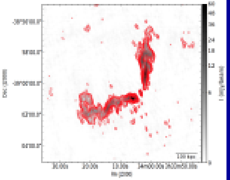

Rotation-invariant CLEANing (Johnston & Hollitt 2016).

Intermezzo:

The Measurement Equation

The Measurement Equation

- Electric field seen by antenna A: $\vec{E^A}$.
- For baseline AB, the coherency matrix is $E^{AB} = \vec{E^A}(\vec{E^B})^H$
- In the α-β polarization basis, the coherency matrix for baseline AB is:

$$E^{AB} = \begin{pmatrix} \left\langle E^A_\alpha \left(E^B_\alpha\right)^* \right\rangle & \left\langle E^A_\alpha \left(E^B_\beta\right)^* \right\rangle \\ \left\langle E^A_\beta \left(E^B_\alpha\right)^* \right\rangle & \left\langle E^A_\beta \left(E^B_\beta\right)^* \right\rangle \end{pmatrix}$$

- The coherency matrix is related to the Fourier transform of the brightness matrix!

$$E^{AB} = \mathcal{F}\left[S\right]\Big|_{(u,v)}$$

- Brightness matrix: For X-Y polarization basis:

$$E^{AB} = \begin{pmatrix} \left\langle E^A_x \left(E^B_x\right)^* \right\rangle & \left\langle E^A_x \left(E^B_y\right)^* \right\rangle \\ \left\langle E^A_y \left(E^B_x\right)^* \right\rangle & \left\langle E^A_y \left(E^B_y\right)^* \right\rangle \end{pmatrix} \quad ; \quad S = \begin{pmatrix} I+Q & U+j\,V \\ U-j\,V & I-Q \end{pmatrix}$$

The Measurement Equation

- Electric field seen by antenna A: $\vec{E^A}$.
- For baseline AB, the coherency matrix is $E^{AB} = \vec{E^A}(\vec{E^B})^H$
- In the α-β polarization basis, the coherency matrix for baseline AB is:

$$E^{AB} = \begin{pmatrix} \left\langle E^A_\alpha \, (E^B_\alpha)^* \right\rangle & \left\langle E^A_\alpha \, (E^B_\beta)^* \right\rangle \\ \left\langle E^A_\beta \, (E^B_\alpha)^* \right\rangle & \left\langle E^A_\beta \, (E^B_\beta)^* \right\rangle \end{pmatrix}$$

- The coherency matrix is related to the Fourier transform of the brightness matrix!

$$E^{AB} = \mathcal{F}\left[S\right]\Big|_{(u,v)}$$

- Brightness matrix: For R-L polarization basis:

$$E^{AB} = \begin{pmatrix} \left\langle E^A_r \, (E^B_r)^* \right\rangle & \left\langle E^A_r \, (E^B_l)^* \right\rangle \\ \left\langle E^A_l \, (E^B_r)^* \right\rangle & \left\langle E^A_l \, (E^B_l)^* \right\rangle \end{pmatrix} \quad ; \quad S = \begin{pmatrix} I+V & Q+j\,U \\ Q-j\,U & I-V \end{pmatrix}$$

Coherency matrix and Visibility matrix.

- Voltage for antenna A with an α-β polarizer is: $\vec{v^A} = J^A \vec{E^A}$, where $\vec{E^A}$ is the electric field in the α-β base and J^A is the Jones matrix that calibrates antenna A.
- The visibility matrix (i.e., voltage cross-correlations) is:

$$V^{AB} = \vec{v_A} \left(\vec{v_B}\right)^H = \begin{pmatrix} \left\langle v_\alpha^A \left(v_\alpha^B\right)^* \right\rangle & \left\langle v_\alpha^A \left(v_\beta^B\right)^* \right\rangle \\ \left\langle v_\beta^A \left(v_\alpha^B\right)^* \right\rangle & \left\langle v_\beta^A \left(v_\beta^B\right)^* \right\rangle \end{pmatrix}$$

- Since $\vec{v_i} = J_i \vec{E_i}$,

$$V^{AB} = J_A \vec{E_A} \left(\vec{E_B}\right)^H J_B^H = J_A \begin{pmatrix} \left\langle E_\alpha^A \left(E_\alpha^B\right)^* \right\rangle & \left\langle E_\alpha^A \left(E_\beta^B\right)^* \right\rangle \\ \left\langle E_\beta^A \left(E_\alpha^B\right)^* \right\rangle & \left\langle E_\beta^A \left(E_\beta^B\right)^* \right\rangle \end{pmatrix} J_B^H$$

Back to HDR Polarimetry

High Dyn. Ranges: Leakage biases

- Effect of the Dterms on the XY^* cross-correlations:

$$XY^* \rightarrow XY^* + D_x^a YY^* + (D_y^b)^* XX^*$$

High Dyn. Ranges: Leakage biases

- Effect of the Dterms on the XY^* cross-correlations:

$$XY^* \rightarrow XY^* + D_x^a YY^* + (D_y^b)^* XX^*$$

- In terms of the brightness matrix (i.e., assuming a point source):

$$XY^* \rightarrow U_{ant} + jV + D_x^a (I - Q_{ant}) + (D_y^b)^* (I + Q_{ant})$$

- Re-arranging terms:

$$XY^* \rightarrow U_{ant} + Q_{ant} \left((D_y^b)^* - D_x^a \right) + jV + I (D_x^a + (D_y^b)^*)$$

Symmetries in Dterm distributions may relate to spurious V and/or m

High Dyn. Ranges: Leakage biases

- $V^{obs} = D_a\, X\, V_{ab}^{true}\, X^H\, D_b^H \quad ; \quad X = \begin{pmatrix} 1 & 0 \\ 0 & e^{j\alpha} \end{pmatrix} \quad ; \quad D_a = \begin{pmatrix} 1 & D_a^L \\ D_a^R & 1 \end{pmatrix}$

$$RL^* \rightarrow ((D_a^R + (D_b^L)^*)\, I + m)\, e^{-j\alpha} + O(D^2)$$
$$LR^* = ((D_a^L + (D_b^R)^*)\, I + m^*)\, e^{j\alpha} + O(D^2)$$

- **Unpolarized** calibrator:
  $(D_a^L,\ D_a^R,\ e^{j\alpha}) \rightarrow (D_a^L\, e^{j\Delta} + jK,\ D_a^R\, e^{-j\Delta} + jK,\ e^{j(\alpha-\Delta)})$

- **Polarized** calibrator:
  $(D_a^L,\ D_a^R,\ e^{j\alpha}) \rightarrow (D_a^L + jK,\ D_a^R + jK,\ e^{j(\alpha)})$

Dterm ambiguities may inject 2nd-order effects in the polarimetry.

Bias in the D-terms?

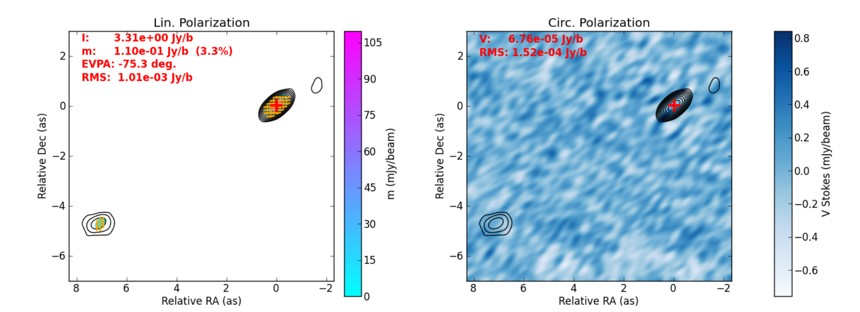

J0522−3627, ALMA Band 5 (172 GHz).
Original calibration.

Bias in the D-terms?

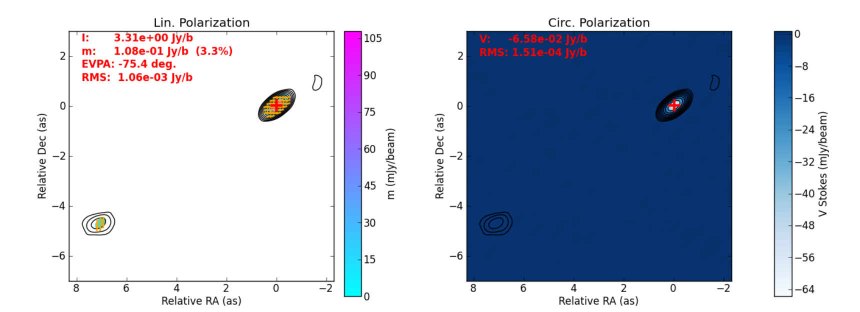

J0522−3627, ALMA Band 5 (172 GHz) with
$D_x \rightarrow D_x + 0.01j$ and $D_y \rightarrow D_y - 0.01j$.

Bias in the D-terms?

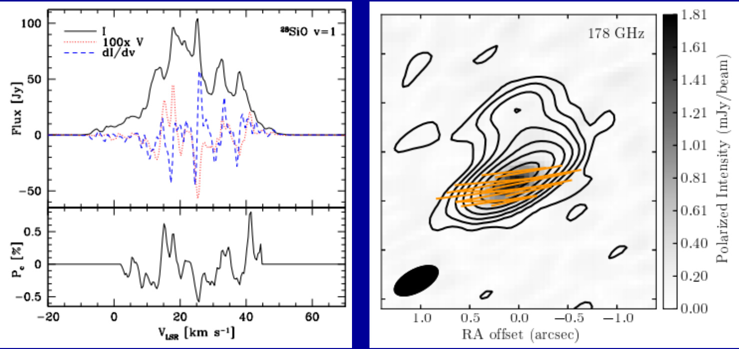

VY CMa, ALMA Band 5 (172 GHz). Spectrum of *V* *not* proportional to *I* (Vlemmings et al. 2017).

High Dyn. Ranges: X-Y phase offset

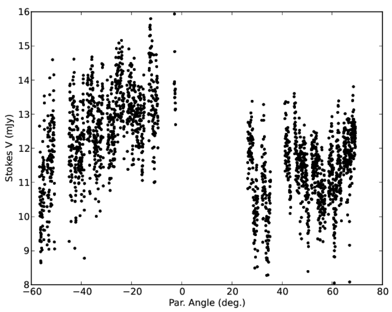

$$V^{spur} \sim V^{true} \cos\Delta + \left(U \sin\left(\phi - \psi\right) + Q \cos\left(\phi - \psi\right)\right) \sin\Delta$$

(e.g., 3C 273 with ALMA @ 1.3 mm; Hovatta et al. in prep.)

High Dyn. Ranges: X-Y phase offset

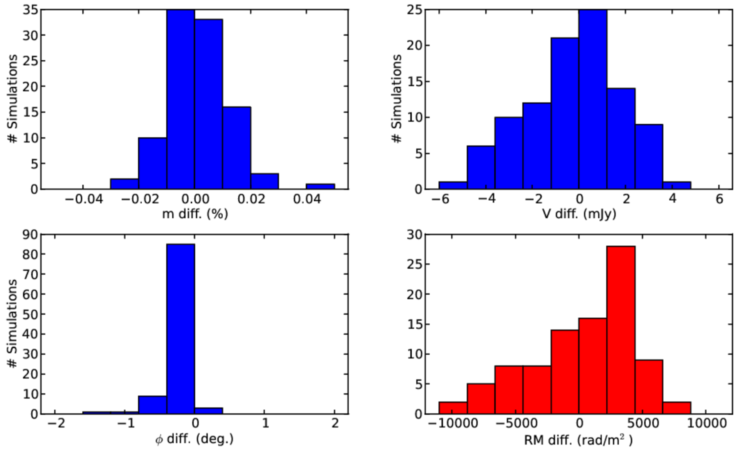

Monte Carlo analysis (e.g., $G \rightarrow D$ cross-talk in 3C273 with ALMA)

High-Sensitivity Polarimetry

High Sensitivities: Intra-field Differential Observables

- The relative brightness within the same observed field is a very precise and accurate quantity (only limited by *dynamic range*).
- Using the relative brightness, we can improve variability analyses by several orders of magnitude.

High Sensitivities: Intra-field Differential Observables

- The relative brightness within the same observed field is a very precise and accurate quantity (only limited by *dynamic range*).
- Using the relative brightness, we can improve variability analyses by several orders of magnitude.
- We need:
  - A source with a resolved structure.

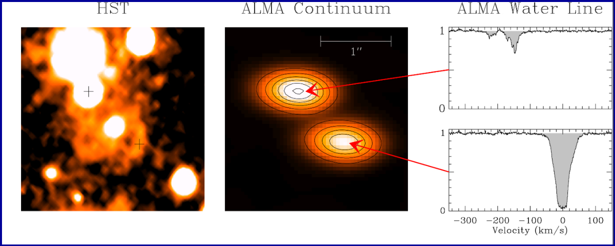

Relative brightness NE/SW

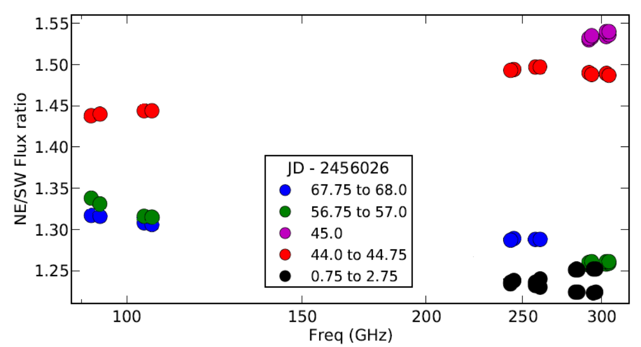

Martí-Vidal et al. (2013)

... and a strong γ-ray counterpart!

CHALMERS
UNIVERSITY OF TECHNOLOGY

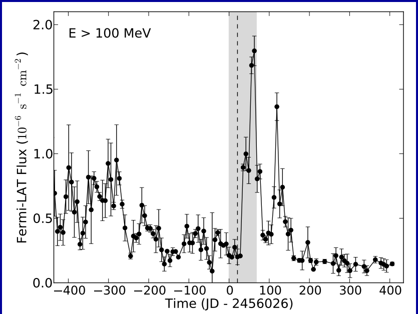

... and a strong γ-ray counterpart!

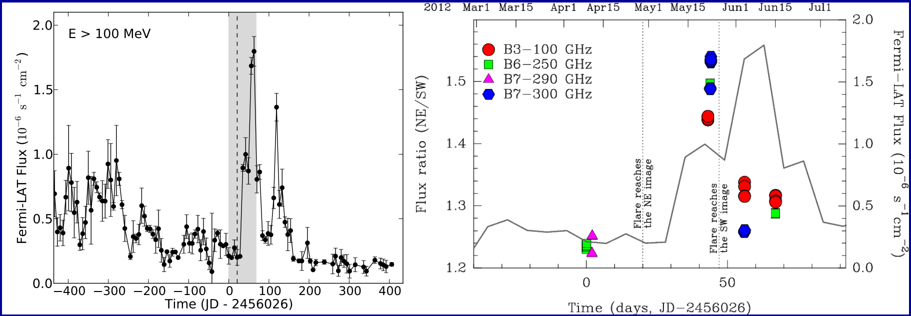

Dual Differential polarimetry NE/SW

- ALMA observed in two polarizations, XX e YY.
- XX is related to the brightness distribution of $I + Q$.
  YY is related to $I - Q$.
- Studying the relative brightness of the XX and YY images, we can extract polarimetry information from the observed source.

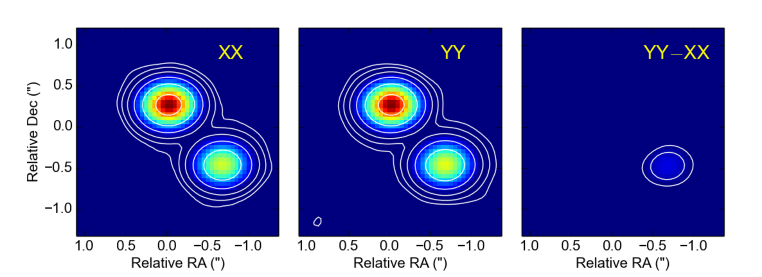

Martí-Vidal et al. (2015)

Dual Differential polarimetry NE/SW

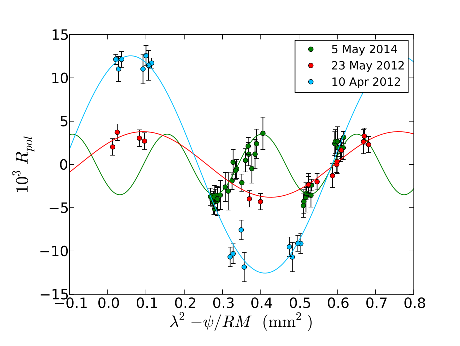

- The largest Faraday rotation so far (*RM* of 3×10^8 rad m^{-1}).
- The highest rest frequencies so far (1 THz, corrected for z). This corresponds to $R \sim 0.01$ pc from the jet base.
- Highest *RM* measured in other AGN (at lower frequencies): $\sim10^6$ rad m^{-1} at 250 GHz (e.g., Plambeck et al. 2014).

More (ALMA) data. 3C 286 (SV @ B6)

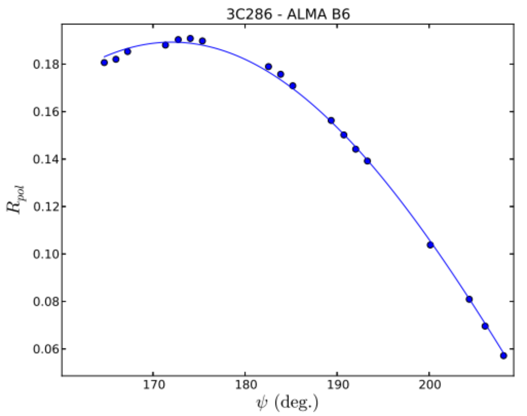

Martí-Vidal et al. *A&A* (2016)

(Result compatible with full-pol calibration: Nagai et al. *ApJ* 2016)

More (ALMA) data. Sgr A* (SV @ B3,6,7)

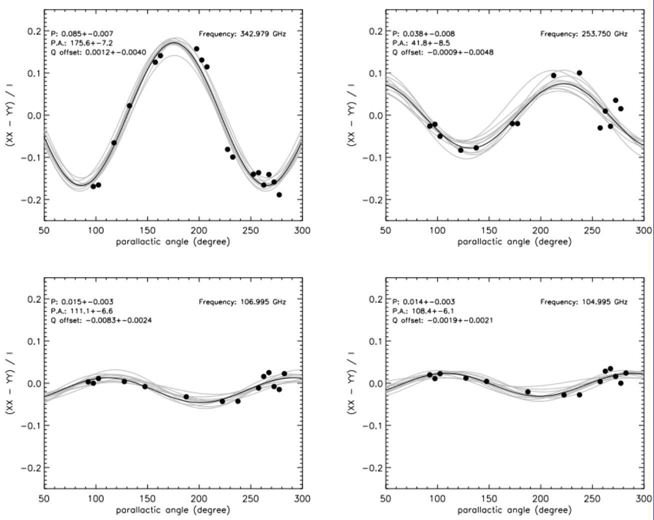

Baobab et al. *A&A* (2016)

Polarimetry at the Highest Angular Resolutions

Highest Angular Resolutions: VLBI

- Limitations of the "Classical" Calibration.
  - Effects of some basic tenets that may not hold. (Marti-Vidal et al. 2012)
- Fractional polarization in Fourier domain.
  - Robust observables independent of deconvolution artifacts. (Johnson et al. 2015)
- Use of wide bandwidths for higher sensitivities.
  - Linear polarizers in VLBI for higher polarization purity (Marti-Vidal et al. 2016).

Classical VLBI Polarization Calibration

- R-L phase stability is assumed.
- Only first-order D-term effects are considered.
- Absolute EVPA is unknown *per sé*.

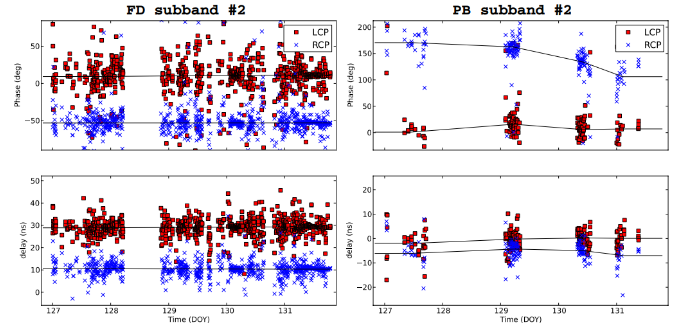

Cross-pol. phases can vary on day timescales (Marti-Vidal et al. 2012)

Classical VLBI Polarization Calibration

- R-L phase stability is assumed.
- Only first-order D-term effects are considered.
- Absolute EVPA is unknown *per sé*.

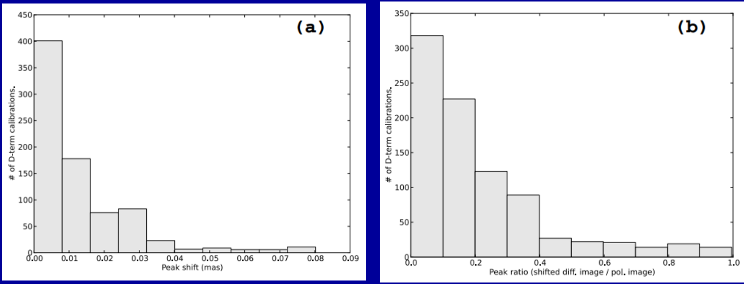

Heavy pol. cutoffs required to deal with residual D-term effects (Marti-Vidal et al. 2015)

Classical VLBI Polarization Calibration

- R-L phase stability is assumed.
- Only first-order D-term effects are considered.
- Absolute EVPA is unknown *per sé*.

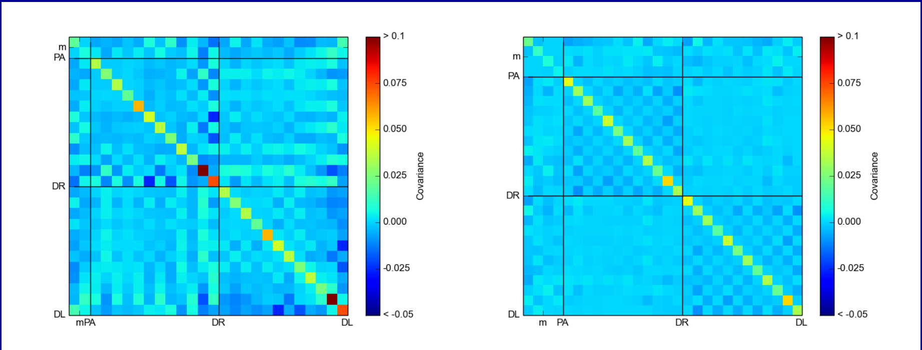

D-term covariance matrix for one calibrator (left) and 2 calibrators (right), with the same total observing time (Marti-Vidal 2016).

Parallactic angle in VLBI

$$P_{xy} = \begin{pmatrix} \cos\phi & -\sin\phi \\ \sin\phi & \cos\phi \end{pmatrix} \qquad P_{rl} = \begin{pmatrix} e^{j\phi} & 0 \\ 0 & e^{-j\phi} \end{pmatrix}$$

- Is the rotation of the antenna mount axis w.r.t. the sky.
- Is deterministic. Apply it before the phase (and delay/rate) calibration!
- It does not commute with the gains for linear polarizers.
- In VLBI, it also mixes V_{xx} and V_{yy} with V_{xy} and V_{yx}.

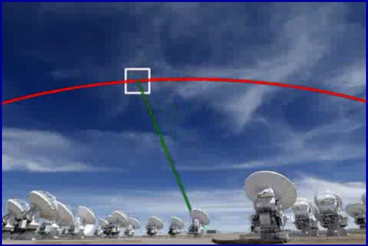

PolConvert

- CASA task for linear-circular conversion (Marti-Vidal et al. 2016).
- Works on either SWIN (i.e., DiFX) or FITS-IDI files.
- Designed for ALMA-VLBI, but already tested on other arrays.
- Either pure linear or mixed-polarization fringes can be handled!

```
CASA <7>: inp
--------> inp()
#  polconvert ::

Version 1.2

Converts VLBI visibilities from mixed-polarization basis (i.e.,
linear-to-circular) into circular basis. Works with single VLBI stations
as well as with phased arrays (i.e., phased ALMA).


IDI                 = '/media/marti/LaCie_3/DATA/APP/VLBA_B3/MPIfR/' #  Input
                                         #   FITS-IDI file with VLBI
                                         #   visibilities. It can  also be a
                                         #   directory containing SWIN files from
                                         #   DiFX.
OUTPUTIDI           = '/media/marti/LaCie_3/DATA/APP/VLBA_B3/MPIfR/' #  Output
                                         #   FITS-IDI file (or SWIN directory).
                                         #   If equal  to IDI, the file(s) will
                                         #   be overwritten
DiFXinput           = '/media/marti/LaCie_3/DATA/APP/VLBA_B3/MPIfR/bm434a_01.input' #  I
                                         #   f SWIN files are being converted,
                                         #   this must  be the *.input file used
                                         #   by DiFX.
doIF                =       [35]         #  List of IFs to convert. Default means
                                         #   all.
linAntIdx           =        [1]         #  List of indices of the linear-
                                         #   polarization  antennas in the IDI
                                         #   file
Range               =         []         #  Time range to convert (integer list;
                                         #   AIPS format).  Default means all
                                         #   data
ALMAvis             = '/home/marti/WORKAREA/ARC/ARC_TOOLS/PolConvert/TEST_DATA/VLBA_B3.m
emmap/CONCAT_spw1.ms' #  I
                                         #   f ALMA has been used, this is the
                                         #   measurement  set with the intra-ALMA
                                         #   visibilities.
spw                 =          0         #  Spectral window in ALMAvis that
                                         #   contains the VLBI band.
calAPP              = '/home/marti/WORKAREA/ARC/ARC_TOOLS/PolConvert/TEST_DATA/VLBA_B3.m
emmap/CALAPPPHASE.tab' #  I
                                         #   f ALMA has been used, this is the
                                         #   combined ASDM_CALAPPPHASE table from
                                         #   the ASDM. The list of measurement
```

```
gains               = [['NONE']]         #  Gain tables to pre-calibrate the
                                         #   linear-pol VLBI  stations (one list
                                         #   of gains per linear-pol station).
dterms              =   ['NONE']         #  D-term tables to pre-calibrate the
                                         #   linear-pol VLBI  stations (one table
                                         #   per linear-pol station).
XYadd               =      [0.0]         #  Add manually a phase between X and Y
                                         #   before  conversion (in deg.). One
                                         #   value per linear-pol station.
swapXY              =    [False]         #  Swap X-Y before conversion. One value
                                         #   per linear-pol  VLBI station.
swapRL              =      False         #  Swap R-L of the OTHER antenna(s) when
                                         #   plotting the fringes.
plotIF              =         35         #  IF index to plot. Default means to
                                         #   NOT plot.
plotRange           = [0, 8, 20, 0, 0, 8, 22, 0] #  Time range to plot (integer
                                         #   list; AIPS format).  Default means
                                         #   to NOT plot
plotAnt             =          2         #  Index of the other antenna in the
                                         #   baseline to plot. Default means to
                                         #   NOT plot.
doTest              =       True         #  If true, only compute (and eventually
                                         #   plot), the data, but leave OUTPUTIDI
                                         #   untouched.

CASA <8>:
```

How does PolConvert Work?

- Linear (or mixed) basis: $V_{+\odot} = \begin{pmatrix} V_{xr} & V_{xl} \\ V_{yr} & V_{yl} \end{pmatrix}$

- Conversion to circular: $V_{\odot\odot} = C_{\odot +} \times G \times V_{+\odot}$
  $C_{\odot +}$ is well known. All we need is to know G!

How does PolConvert Work?

- Linear (or mixed) basis: $V_{+\odot} = \begin{pmatrix} V_{xr} & V_{xl} \\ V_{yr} & V_{yl} \end{pmatrix}$

- Conversion to circular: $V_{\odot\odot} = C_{\odot+} \times G \times V_{+\odot}$
  $C_{\odot+}$ is well known. All we need is to know G!

- How does G look like? $\rightarrow G = \begin{pmatrix} 1 & 0 \\ 0 & \rho \end{pmatrix}$
  where ρ is the cross-polarization gain, i.e G_Y/G_X.

- In the basis of circular polarizers:
  $V_{\odot\odot}^{cal} \propto \begin{pmatrix} 1 & D \\ D & 1 \end{pmatrix} \times V_{\odot\odot}^{obs}$, where $D = \dfrac{1-\rho}{1+\rho}$

Calibration Approach (non-ALMA)

Global *Cross-Polarization* Fringe Fitting (Martí-Vidal et al. 2016):

$$\min\left[\chi^2(\vec{\rho})\right] \text{ with } \chi^2(\vec{\rho}) = \sum_k (RR_k/LL_k - 1)^2 + \lambda \left[\sum_k \left(RL_k^2 + LR_k^2\right)\right]$$

Calibration Approach (non-ALMA)

Global *Cross-Polarization* Fringe Fitting (Martí-Vidal et al. 2016):

$$\min\left[\chi^2(\vec{\rho})\right] \text{ with } \chi^2(\vec{\rho}) = \sum_k (RR_k/LL_k - 1)^2 + \lambda\left[\sum_k (RL_k^2 + LR_k^2)\right]$$

$$\chi^2 = \chi^2_{+\odot} + \chi^2_{\odot\odot} \text{ with } \chi^2_{+\odot} = \sum_k \omega_k \left[\frac{V^k_{xr}\rho_+^{-1} - jV^k_{yr}}{V^k_{xl}\rho_+^{-1} + jV^k_{yl}}(e^{\psi_+})(e^{\psi^*_\odot})(\rho_\odot^{-1})^* - 1\right]^2$$

Calibration Approach (non-ALMA)

Global *Cross-Polarization* Fringe Fitting (Martí-Vidal et al. 2016):

$$\min\left[\chi^2(\vec{\rho})\right] \text{ with } \chi^2(\vec{\rho}) = \sum_k (RR_k/LL_k - 1)^2 + \lambda\left[\sum_k \left(RL_k^2 + LR_k^2\right)\right]$$

$$\chi^2 = \chi^2_{+\odot} + \chi^2_{\odot\odot} \text{ with } \chi^2_{+\odot} = \sum_k \omega_k \left[\frac{V^k_{xr}\rho_+^{-1} - jV^k_{yr}}{V^k_{xl}\rho_+^{-1} + jV^k_{yl}}(e^{\psi_+})(e^{\psi^*_\odot})(\rho_\odot^{-1})^* - 1\right]^2$$

- The idea is to derive all the cross-polarization gain ratios in one shot (for both linear and circular polarizers).
- This approach is independent of the source structure!
- And you can get the absolute EVPA calibration for free!!!

GMVA (W Band; ON in linear)

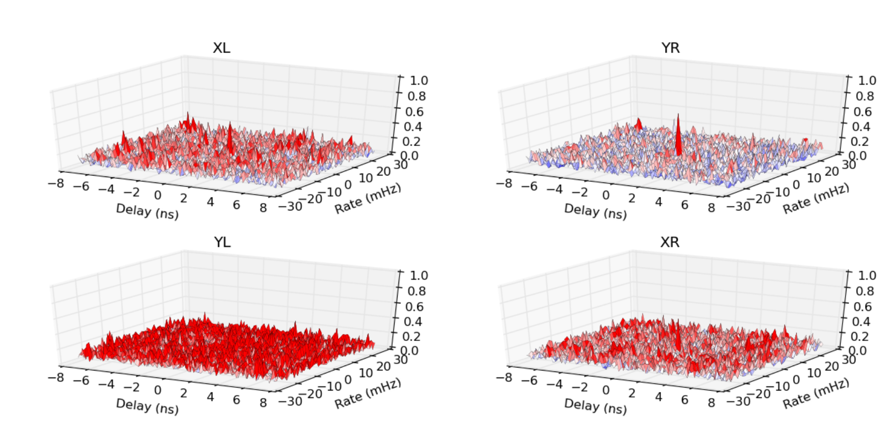

Onsala to Effelsberg (10 sec. on OJ 287)

GMVA (W Band; ON in linear)

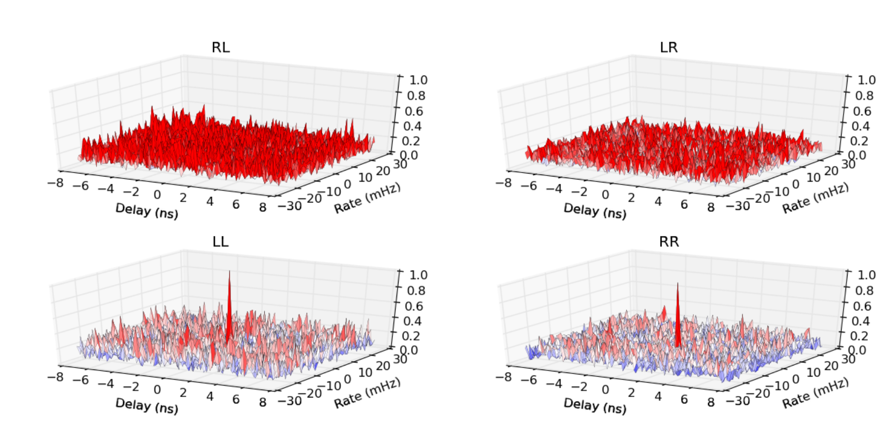

Onsala to Effelsberg (10 sec. on OJ 287)

eEVN (C Band; EB in linear)

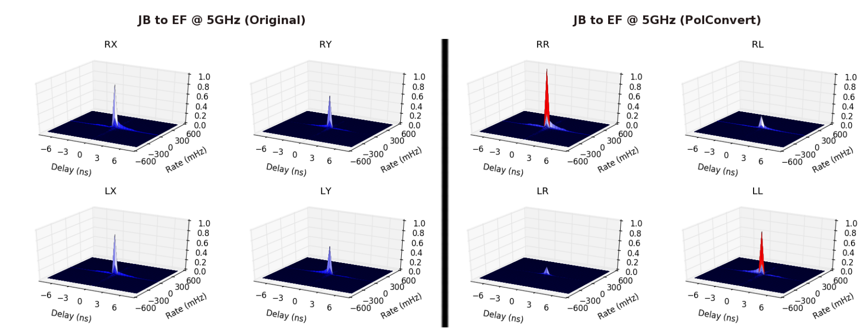

(EO014, PI: M. Olech)

eEVN (C Band; EB in linear)

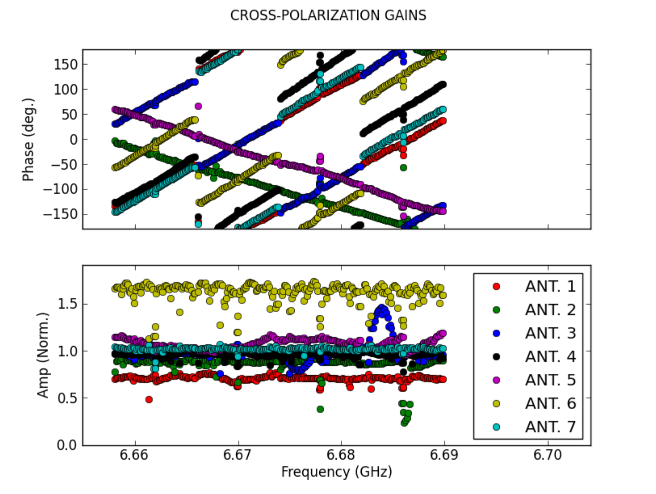

GCPFF! Effelsberg (Ant. 2) is in green

ATCA-KVN (Q/W bands; AT in linear)

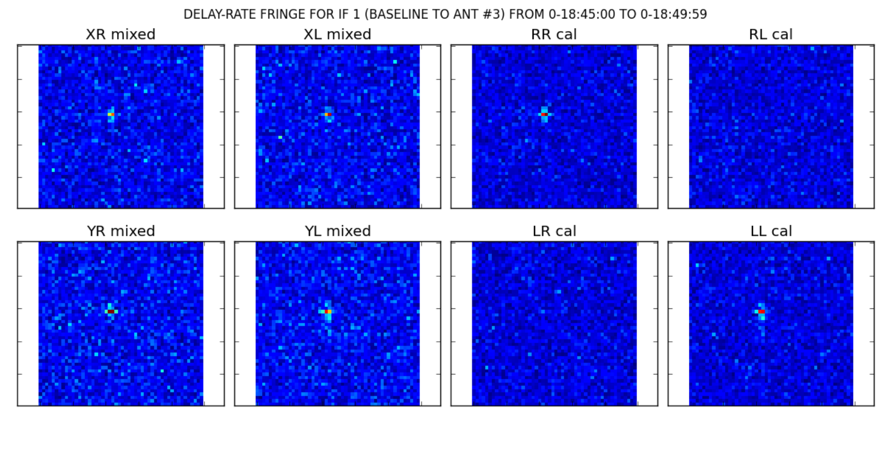

Chanapote (PI of data) & Dodson

LBA (C Band; AT in linear)

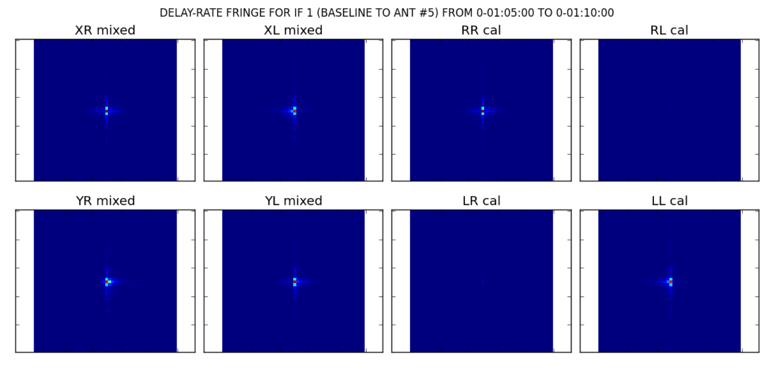

Chanapote (PI of data) & Dodson

LBA (C Band; AT in linear)

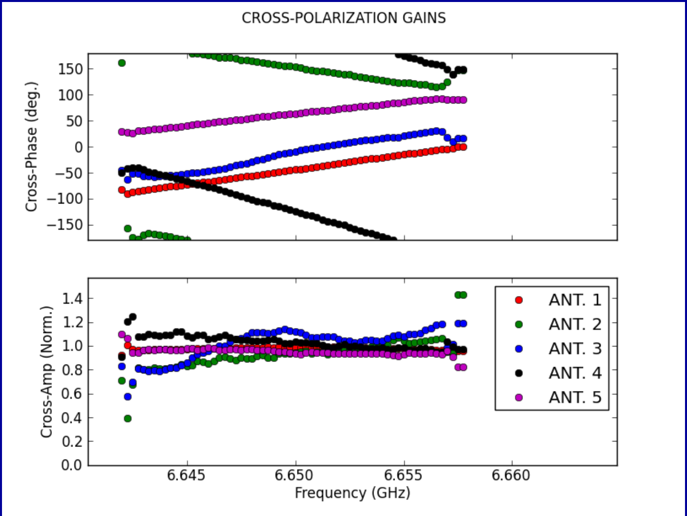

GCPFF! ATCA in red

LBA (C Band; AT in linear)

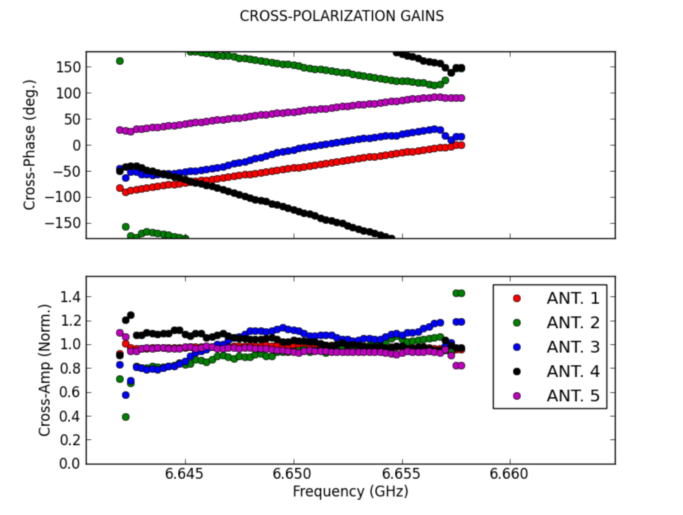

If used on Mopra → D-terms would lower from $15 - 20\%$ ($\pi/2$ plates) to $3 - 5\%$.

ALMA-LMT @ B6 (230 GHz)

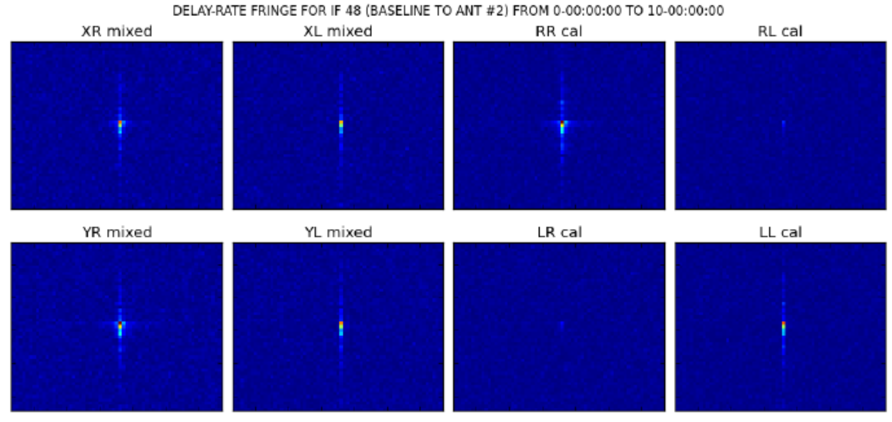

ALMA to LMT (México)

ALMA-LMT @ B6 (230 GHz)

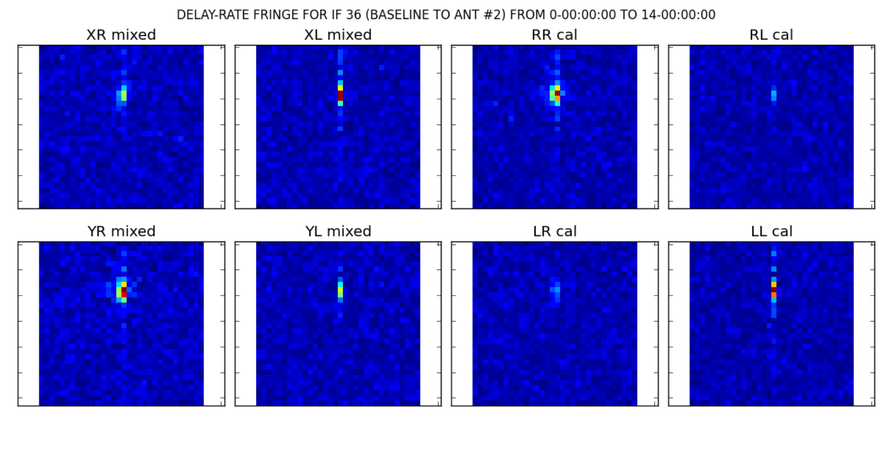

ALMA to LMT (México)

Fractional Polarization in UV Domain

$$\frac{\langle L_1 R_2^* \rangle}{\langle L_1 L_2^* \rangle} \approx \left(\frac{G_{2,\mathrm{R}}}{G_{2,\mathrm{L}}}\right)^* \left[\breve{m}^*(-\mathbf{u}_{12}) e^{2i\phi_2} + D_{1,\mathrm{L}} e^{-2i(\phi_1-\phi_2)} + D_{2,\mathrm{R}}^*\right]$$

$$\frac{\langle L_1 R_2^* \rangle}{\langle R_1 R_2^* \rangle} \approx \left(\frac{G_{1,\mathrm{L}}}{G_{1,\mathrm{R}}}\right) \left[\breve{m}^*(-\mathbf{u}_{12}) e^{2i\phi_1} + D_{1,\mathrm{L}} + D_{2,\mathrm{R}}^* e^{2i(\phi_1-\phi_2)}\right]$$

$$\frac{\langle R_1 L_2^* \rangle}{\langle L_1 L_2^* \rangle} \approx \left(\frac{G_{1,\mathrm{R}}}{G_{1,\mathrm{L}}}\right) \left[\breve{m}(\mathbf{u}_{12}) e^{-2i\phi_1} + D_{1,\mathrm{R}} + D_{2,\mathrm{L}}^* e^{-2i(\phi_1-\phi_2)}\right]$$

$$\frac{\langle R_1 L_2^* \rangle}{\langle R_1 R_2^* \rangle} \approx \left(\frac{G_{2,\mathrm{L}}}{G_{2,\mathrm{R}}}\right)^* \left[\breve{m}(\mathbf{u}_{12}) e^{-2i\phi_2} + D_{1,\mathrm{R}} e^{2i(\phi_1-\phi_2)} + D_{2,\mathrm{L}}^*\right]$$

$$\frac{\langle R_1 R_2^* \rangle}{\langle L_1 L_2^* \rangle} \approx \left(\frac{G_{1,\mathrm{R}}}{G_{1,\mathrm{L}}}\right) \left(\frac{G_{2,\mathrm{R}}}{G_{2,\mathrm{L}}}\right)^* e^{-2i(\phi_1-\phi_2)}.$$

Based on cross-polarization visibility ratios. Robust observables (Johnson et al. 2015)

Fractional Polarization in UV Domain

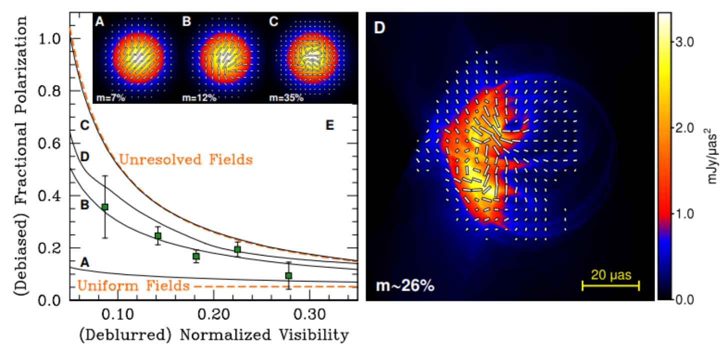

Model-independent quantities related to polarization substructures!
(Johnson et al. 2015)

SUMMARY

- New observational windows are opening in interferometry: wider bandwidths, higher sensitivities, and higher image fidelities (dynamic ranges).
- New algorithms are being developed to squeeze the instrumentation capabilities.
- We summarize some examples of advanced algorithms in interferometric polarimetry:
  - Wide-bandwidth polarimetry → RM reconstruction in Faraday space.
  - High Dynamic Range → Primary-beam modelling, RI-CLEAN, ...
  - High Sensitivity → Differential observables.
  - High Angular Resolution (VLBI) → High-precision D-term estimates from multi-calibrator observations, fractional polarization in UV space, linear polarizers (PolConvert).

SUMMARY

- New observational windows are opening in interferometry: wider bandwidths, higher sensitivities, and higher image fidelities (dynamic ranges).
- New algorithms are being developed to squeeze the instrumentation capabilities.
- We summarize some examples of advanced algorithms in interferometric polarimetry:
  - Wide-bandwidth polarimetry → RM reconstruction in Faraday space.
  - High Dynamic Range → Primary-beam modelling, RI-CLEAN, ...
  - High Sensitivity → Differential observables.
  - High Angular Resolution (VLBI) → High-precision D-term estimates from multi-calibrator observations, fractional polarization in UV space, linear polarizers (PolConvert).

THANKS